Separation of double-electron and atomic XAFS contributions in x-ray absorption spectra of Pt foil and $Na_2Pt(OH)_6$

2002 J. Phys.: Condens. Matter 14 13529

(http://iopscience.iop.org/0953-8984/14/49/309)

INSTITUTE OF PHYSICS PUBLISHING JOURNAL OF PHYSICS: CONDENSED MATTER

J. Phys.: Condens. Matter **14** (2002) 13529–13541 PII: S0953-8984(02)35417-1

Separation of double-electron and atomic XAFS contributions in x-ray absorption spectra of Pt foil and $Na_2Pt(OH)_6$

G E van Dorssen[1], D C Koningsberger[1] and D E Ramaker[2]

[1] Department of Inorganic Chemistry, Debye Institute, Utrecht University, PO Box 80083, 3508 TB Utrecht, The Netherlands
[2] Department of Chemistry and Materials Science Institute, George Washington University, Washington, DC 20052, USA

Received 4 April 2002, in final form 22 October 2002
Published 29 November 2002
Online at stacks.iop.org/JPhysCM/14/13529

Abstract

Both double-electron excitation (DEE) and atomic XAFS (AXAFS) contributions are shown to be present in L_{23} x-ray absorption spectra of Pt foil and $Na_2Pt(OH)_6$. In the Fourier transform of the spectra, the DEE feature appears at lower R values than the AXAFS feature. A background subtraction procedure is developed that leaves the DEE contribution in the background and the AXAFS in the oscillatory part of the spectrum. The separation of the DEE and the AXAFS contributions is possible only when using a cubic spline function routine in which the smoothing parameter can be continuously adjusted.

1. Introduction

The total absorption $\mu(k)$ in an x-ray absorption spectrum (XAS) is commonly defined relative to the atomic x-ray absorption coefficient $\mu_0(k)$, as $\mu(k) = \mu_0(k)(1 + \chi_{EX})$, with $\mu_0(k)$ the atomic background and χ_{EX} the extended x-ray absorption fine structure (EXAFS) function. In the conventional analysis, the atomic background is assumed to be smooth and non-oscillatory. However, several authors [1–3] have recently shown that this is not necessarily true, and the exact cause for this has been controversial.

It was first shown by Holland *et al* [1] that a fine structure in $\mu_0(k)$ can be observed: $\mu_0(k) = \mu_{\text{free}}(k)(1 + \chi_{AX})$, with μ_{free} the free atomic background. This fine structure (χ_{AX}) was attributed to atomic XAFS (AXAFS). The fine structure was assumed to be caused by the scattering of the photoelectron, in the periphery of the absorbing atom, against the potential barrier of the embedded atom potential. However, Filipponi and Di Cicco [4] ascribe the background structures to multiple-or double-electron excitations (DEEs). Di Cicco and Filipponi [5] measured the absorption spectra for several sixth period elements, and compared the resulting structure in the atomic background signal with SCF Dirac–Fock calculations.

They concluded that the structure is caused by DEE involving the 4f electrons, and that it can also produce a contribution at low R in the Fourier transform (FT).

Considerable evidence has accumulated in the literature in favour of the assignment of the low R contribution in the FT to the presence of AXAFS. For the materials used in their study, Rehr *et al* [2] concluded that the AXAFS is quite large, and probably exceeds the DEE effects in magnitude. The authors extracted the atomic background absorption in the Ba, Ce and Pr K-edge XAFS data for $PrBa_2Cu_3O_7$, CeO_2 and BaO respectively using an iterative background removal procedure and then compared the experimental background with *ab initio* calculations of the atomic background. They found that the AXAFS oscillatory fine structure in the background could be approximated by an expression

$$\chi_{AX} = -\frac{1}{kR_{mt}^2}|f_{AX}|\sin(2kR_{mt} + 2\delta_l^a + \Phi_{AX}), \tag{1}$$

where $f_{AX} = |f_{AX}|\exp(i\Phi_{AX})$ is the effective curved-wave scattering amplitude of the interstitial charge density, δ_l^a the central atom phase shift and R_{mt} the muffin-tin radius of the absorbing atom. Equation (1) is analogous to the one used in conventional XAFS analysis; however, the AXAFS oscillations have longer wavelength compared to the EXAFS oscillations because of the smaller effective R. Rehr *et al* [6] further showed that this background structure could be calculated using their FEFF code, with the results in reasonably good agreement with the experimental background. In other work, Wende *et al* [7] concluded from their analysis of SEXAFS data for N on Cu(100) and Cu(110) surfaces that the complication of DEE does not exist in their data, because their absorber atoms had very low atomic number.

The changes observed recently at low R values in the FT with small chemical changes in the system provide further evidence that this region is dominated by the AXAFS contribution. Such changes would not be expected if the DEE contributions dominated the FT at low values of R. O'Grady *et al* [8] measured XAS spectra of Pt–Ru alloys with different compositions and of an *in situ* Pt electrode at different electrode potentials. They used a background subtraction procedure that, in contrast to Rehr, leaves the AXAFS signal in the oscillatory XAFS spectrum. The low R intensity in the FT was found to systematically change proportional to the applied electrode potential. Such a change would not be expected from DEE contributions. Further chemical effects on the intensity and position of the FT-AXAFS have been shown recently for supported small platinum particles [9–12]. The FT-AXAFS peaks of supported platinum particles are strongly dependent on the properties of the support. The changes in the amplitude and position of the FT-AXAFS peaks can be attributed to changes in charge density of the support oxygen ions as a function of the support acidity/alkalinity, number of protons, type of charge compensating cation and the presence of extra-framework aluminium. Finally Ramaker *et al* [13] have shown that changes in the cation, M^+, in the anion–cation pair $Zn(OH)_4{}^{2-}$–$(H_2O)_nM^+$ induced strong changes in the Zn K-edge FT-AXAFS contribution on the anion. These experimental results provide strong evidence that the FT-AXAFS can be used to probe chemical effects, even those resulting from chemical changes two and three atom shells removed from the absorber. Further, such changes would not be expected to occur in the DEE contributions. Thus these changes in the low R region of the FT must be due to the dominant FT-AXAFS contribution. From all the results discussed above, it is clear that AXAFS is present, but there still exists a controversy whether the structures at low R values in the FT spectra are exclusively caused by AXAFS, or also partly by DEE.

In this paper it will be shown that both DEE and AXAFS contributions are indeed present in the x-ray absorption spectra of Pt foil and $Na_2Pt(OH)_6$, and that they can be distinguished and separated. A background subtraction procedure is developed which separates the AXAFS (and regular EXAFS) from the DEE contribution, leaving the DEE in the background and

placing the AXAFS in the oscillatory EXAFS function. Since Pt is an element with a large atomic number, the existence of DEE contributions in this case is not too surprising. Whether separating the DEE and AXAFS is possible in most other experimental XAFS spectra remains to be determined, but in this paper some evidence from modelling is presented that this will generally be the case.

2. Experimental and methods

Measurements have been performed on Pt foil and $Na_2Pt(OH)_6$ to provide experimental data for Pt–Pt and Pt–O scatterer pairs respectively. The Pt and $Na_2Pt(OH)_6$ sample thicknesses were chosen to have an absorption of $\Delta\mu x = 1.0$ in order to minimize thickness effects. Both samples were measured at liquid nitrogen temperature. The data were collected in transmission mode on wiggler station 9.2 of the Daresbury SRS, which is equipped with a Si(220) plane double-crystal monochromator. Higher harmonics were suppressed by detuning the monochromator to 50% of the total intensity at the Pt L_3 edge (11 564 eV). Two ionization chambers were used, filled with argon so that μx is 20% in the first ion chamber and 80% in the second ionization chamber. The estimated energy resolution, determined by the vertical beam size, was 3.5 eV at the Pt L_3 edge.

The pre-edge background of the XAFS spectra was approximated by a modified Victoreen curve and normalization was carried out by dividing the absorption spectrum by the height of the absorption edge at 50 eV above the edge [14]. The background is approximated by a spline function defined by

$$\sum_{i=1}^{NPTS} \frac{(\mu_i - BCK_i)^2}{\mathrm{e}^{-WEk_i^2}} \leqslant \mathrm{SM}. \tag{2}$$

The criteria used in the past for background removal were based on the procedure first outlined by Cook and Sayers [15]. If SM is set to zero, the background goes through all the experimental points, and no EXAFS structure remains. Increasing the value of SM smoothes out the background and leaves more structure in the EXAFS function. In general this structure is best characterized in the FT of the EXAFS, $\mathrm{FT}(\chi_{EX})$, which reveals peaks at various R values. Historically, the criteria utilized decreased SM until all of the features below 1.5 Å in the FT were extracted from the FT (we denote this in the following as the $\mathrm{SM}_{R<1.5}$ criterion). In most cases the $\mathrm{SM}_{R<1.5}$ criterion led to a small decrease (10%) of the first shell EXAFS peak.

The isolation of the AXAFS and EXAFS signals from the smooth free atom background is important for a proper analysis of both AXAFS and EXAFS phenomena. In previous papers dealing with the analysis of AXAFS spectra [9–12] we have defined new criteria:

- Diminish as much as possible the contribution at $R < 0.5$ Å.
- Make sure the EXAFS intensity at $R > 1.5$ Å is unchanged.
- Check both k^1 and k^3 weighted spectra, for different k ranges, including low k values.

The last criterion is important to ensure that no EXAFS signal is removed from the raw data. These new criteria will be denoted in the following by the $\mathrm{SM}_{R<0.5}$ criterion. The spline function as given in equation (2) is used for the background removal, with the weight parameter WE set to zero. The spline functions for the background are therefore determined exclusively by the smoothing parameter SM.

3. Results

3.1. Separation of DEE from the AXAFS and EXAFS

In order to investigate the origin of the FT peaks at low values of $R(R < 1/2R_{\mathrm{Pt-Pt}})$, the FT ($k^1$, $\Delta k = 1.5$–12 Å^{-1}) of Pt foil is plotted in figure 1(a) for different characteristic values of the smoothing parameter SM (dotted curve, 3.5; solid curve, 3.4; dashed curve, 3.3; dashed–dotted curve, 3.2). The obtained results can be visually distinguished for changes in SM values smaller than 0.05. Therefore, the uncertainty in the values of SM is estimated to be 0.02. On a more expanded scale (figure 1(b)) it can be seen that three main low R peaks ($R = 0.18$, 0.78 and 1.12 Å) can be distinguished. The first shell Pt–Pt peak ($R = 2.46$ Å) is also displayed on an expanded scale in figure 1(c). It is possible to determine the intensities of the above mentioned peaks as a function of the SM parameter. In figure 2, the intensity of each R peak is normalized to the intensity of the FT peak obtained with an SM value of 3.7. The intensity at $R = 0$ Å is due to the presence of atomic background in the FT. It can be seen in figure 2 that the intensity at $R = 0$ Å and the peak at $R = 0.18$ Å strongly decreases with SM for $3.7 > \mathrm{SM} > 3.4$ compared with a much slower decrease for the peaks at 0.78 and 1.12 Å. The intensity of the Pt–Pt peak decreases by only a few per cent in this range of SM values.

By plotting the background for the different characteristic values of the SM parameters it is now possible to identify the FT peaks at low values of R. A smooth parameter value of 3.5 leads to a smooth background (see figure 3). Decreasing the smooth parameter to a value of 3.4 gives an oscillation at low energy (node around 40 eV) and a more steplike function around 160 eV. At the same time the peak at 0.18 Å in the FT disappeared and a constant intensity at this value of R is observed for smaller SM values. Di Cicco and Filipponi [5] calculated that the onset energy of the [2p4f] DEE for Pt is at approximately 110 eV with the contribution maximizing around 175 eV. The steplike feature visible in the background maximizes at approximately this energy (see figure 3). Therefore this steplike feature can be assigned to the opening of the [2p4f] DEE channel. In the SM = 3.5 background, on the other hand, this feature is missing. This feature is now present in the separated XAFS oscillations and visible in the FT at 0.18 Å. Based upon our earlier AXAFS studies [9–12] the peak at 1.12 Å can be attributed to AXAFS. The dependence of the decrease of the peaks at 0.78 and 1.12 Å on SM in the range $3.5 > \mathrm{SM} > 3.2$, as shown in figure 2, gives a strong indication that the peak at 0.78 Å originates both from DEE and AXAFS.

In our previous AXAFS studies we have used the earlier mentioned $\mathrm{SM}_{R<0.5}$ criterion. The goal of this work is to determine whether this criterion indeed leaves the DEE contribution in the background and the AXAFS contribution in the FT. Figure 2 makes clear that this tasks is essentially accomplished if it can be shown that the DEEs contribute mainly to the structure below $R = 0.5$ Å and that the peak around 0.2 Å is not largely mixed with AXAFS. To show this a model spectrum is generated by fitting the experimental Pt foil L_3 absorption edge step with an arctangent function and adding a DEE contribution with a width Γ,

$$\mu = a + b \cdot E + \arctan\left(\frac{E}{\Delta}\right) + \mathrm{DEE} * \Gamma. \tag{3}$$

Here, a and b are parameters to best model the smooth background, and Δ is the width of the absorption edge. The decay parameter b is chosen so that the post-edge of the simulated absorption follows the post-edge decay of a Pt–H absorption calculated by FEFF7 (see below). The [2p4f] DEE contribution is generated, based on [5], by taking a flat contribution with step height of 0.005 (this is approximately the intensity Di Cicco and Filipponi found). The step is broadened to about 50 eV total width before this function is added to the smooth background

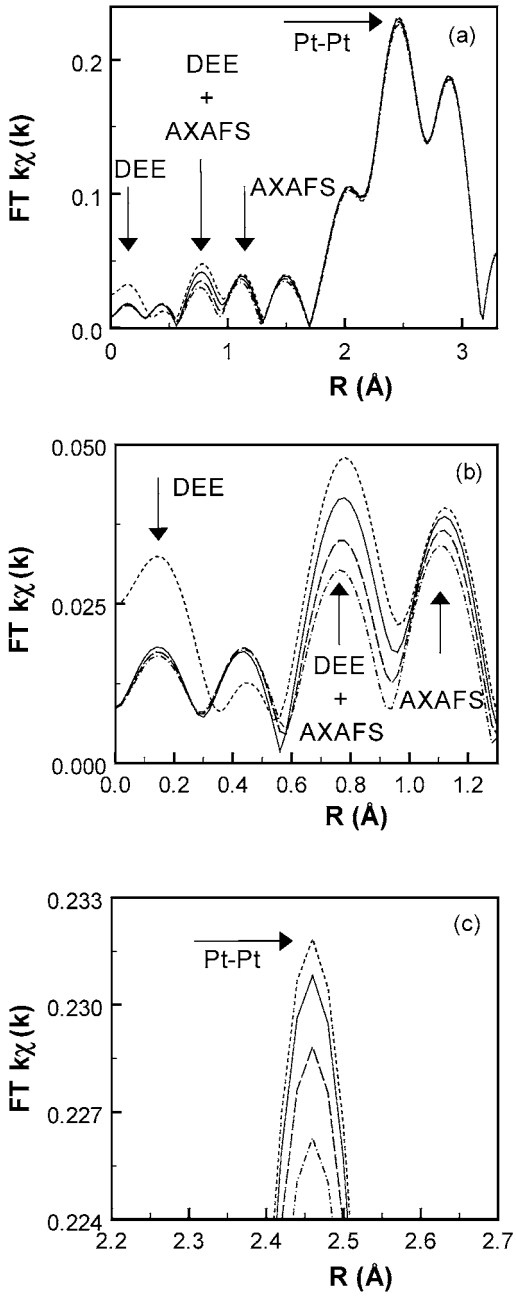

Figure 1. (a) FT (k^1, Δk = 1.5–12 Å^{-1}) of the Pt foil XAFS data for different characteristic values of the smooth parameter SM (dotted curve, 3.5; solid curve, 3.4; dashed curve, 3.3; dashed dotted curve, 3.2). The origin of the different peaks is indicated; DEE: double electron excitations, AXAFS: atomic XAFS. and Pt–Pt: first shell Pt–Pt peak. (b) Same as in (a) but with an expansion in the low *R* region. (c) Same as in (a) but with an expansion in the *R* region containing the first shell Pt–Pt peak.

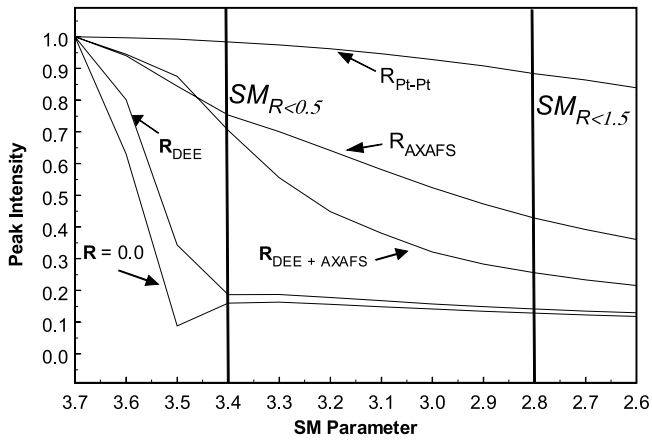

Figure 2. Intensity of the various FT peaks as a function of the smoothing parameter (SM). The dominant contribution of each peak is indicated. The two different SM_R criteria are also indicated by the vertical lines.

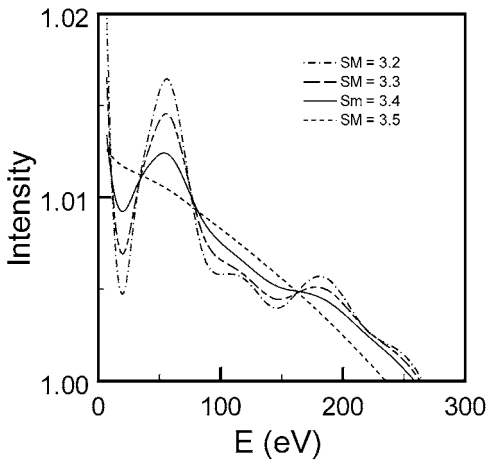

Figure 3. Background of Pt foil XAFS data as a function of the smoothing parameter (SM): dotted curve, 3.5; solid curve, 3.4; dashed curve, 3.3; dashed–dotted curve, 3.2.

spectrum. The position of the onset of the DEE structure was set at about 140 eV. This energy corresponds to the onset of the steplike feature that can be seen in figure 3.

This total model spectrum was background subtracted using the same criterion ($SM_{R<0.5}$, DEE in background, or $SM_{R=0.0}$, DEE in FT) as for the experimental data. The resulting background and corresponding FT spectra are shown in figures 4(a) and (b). The maximum in the FT due to the DEE feature is located around $R = 0.3$ Å implying that the structures present for $R < 0.5$ Å in the FT spectrum of Pt foil (see figure 1(b)) are indeed due to the DEE contribution.

This model spectrum can now be varied at will to determine the generality of this last conclusion, i.e. whether the FT-DEE peak always appears at $R < 0.5$ Å. The width and position of the FT-DEE spectrum of course does depend on the parameters in the model spectrum, but the primary FT-DEE contribution generally stays well below $R < 0.5$ Å with

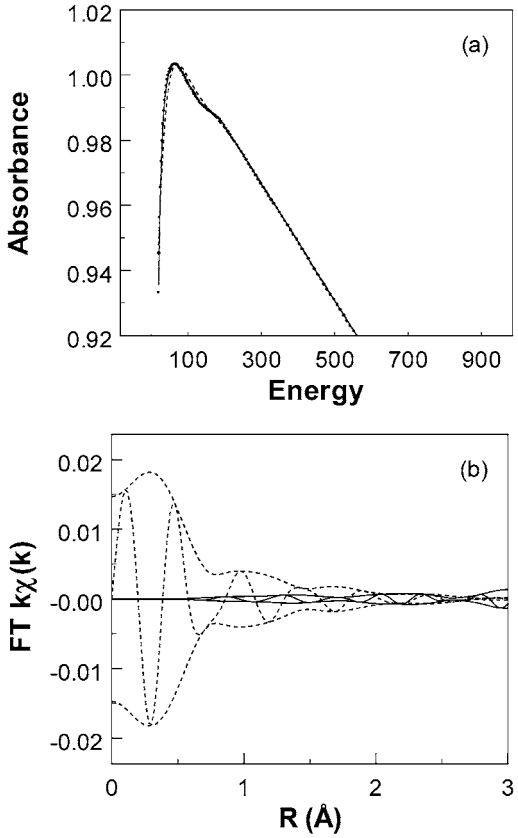

Figure 4. (a) Free atom background (solid curve) and the background extracted with $SM_{R=0.0} = 0.1$ (dashed curve) and $SM_{R<0.5} = 0.0005$ (dots). The solid and dashed curves are essentially indistinguishable. (b) FT (k weighted, $k = 2.0$–18 Å^{-1}) of remainder χ after background removal of simulated spectrum (solid curve, $SM_{R<0.5} = 0.0005$; dashed curve, $SM_{R=0.0} = 0.1$). Note the difference in amplitude due to the FT range.

a small contribution under the $R = 0.8$ peak, its magnitude depending on the width Γ and onset energy. This also shows that the peak at 0.78 Å in figure 1(b) is indeed composed of two contributions (DEE and AXAFS).

From the results given above it can be concluded that an SM value of 3.4 satisfies the earlier used $SM_{R<0.5}$ criterion. As can be seen in figure 3 a further decrease of the SM parameter leads to the appearance of more oscillations in the background, partly due to AXAFS and the first shell Pt–Pt EXAFS. The appropriateness of SM = 3.4 for Pt foil is clearly visible from figure 5. It compares the background for SM = 3.4 with the isolated AXAFS (see below), and a scaled down total Pt–Pt EXAFS spectrum (including higher shells). This comparison shows that the background obtained with an SM value of 3.4 contains the DEE contribution. There is no sign of any AXAFS structure. However, the decrease in the AXAFS peak at 1.18 Å is in fact 7% (see figure 1(b)). The structure below 75 eV in figure 3 is due to the first shell Pt–Pt. The intensity of the first shell Pt–Pt peak is about five times larger than the peaks at low R due to DEE and AXAFS. A decrease by only 4% (see figure 1(c)) of the FT first shell Pt–Pt peak will be visible as a first shell Pt–Pt oscillation in the background. The $SM_{R<0.5}$ and $SM_{R<0.0}$ criteria were also used for subtracting the background from the XAFS data of $Na_2Pt(OH)_6$.

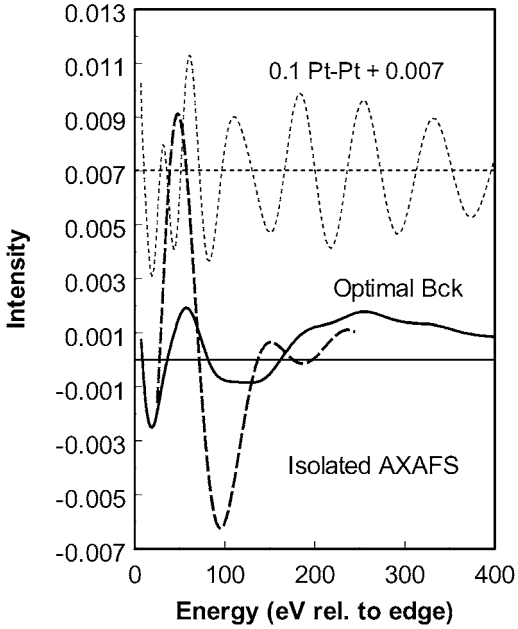

Figure 5. Comparison of the optimal background ($SM_{R<0.5} = 3.4$) for Pt foil with the isolated AXAFS (see text and figure 8), and the Pt–Pt first shell EXAFS function, reduced and shifted as indicated for clarity.

The results are shown in figures 6(a) and (b). It can be seen in figure 6(b) that the $SM_{R<0.5}$ criterion brings the DEE into the background.

To further verify our background removal procedure, a comparison can be made between the free atom backgrounds obtained from the Pt foil and $Na_2Pt(OH)_6$ XAFS data and a calculated free atom background. The experimental free atom backgrounds are obtained by moving both the DEE and AXAFS into the oscillatory part of the XAFS data and removing them fully from the background. The free atom background has been simulated by calculating the total absorption spectrum, μ, for one H atom and one Pt atom at a reasonably large distance, in this case[3] $R = 2.6$ Å. Assuming the AXAFS and EXAFS contributions are negligible in this case, μ then directly estimates μ_{free}. A free atom background has also been calculated for a Pt_{55} and a PtO_6 cluster. It can be seen in figure 7 that the theoretically generated backgrounds and the experimental backgrounds obtained from the Pt foil and $Na_2Pt(OH)_6$ XAFS data are in general good agreement.

3.2. Separation of AXAFS from EXAFS

In order to isolate the AXAFS from the normal EXAFS the first shell Pt–Pt or Pt–O peaks were fitted in R space using the XDAP [16] program. Theoretical phase and backscattering amplitudes for the Pt–Pt and Pt–O scattering pairs were generated utilizing the FEFF7 [6] code. However, the FEFF7 code allows several choices of potential types and parameters. The potential type, the real and imaginary parameters which specifically characterize this potential, $S_0{}^2$ and the Debye–Waller factor were all varied in FEFF7 until the generated

[3] The FEFF parameters utilized here have been optimized as described elsewhere (see [10] and [12]). Briefly, the Dirac–Hara potential was used with V_r and V_i chosen to be -4.2 and 3 eV for Pt–Pt, and 0.0 and 3 eV for Pt–O.

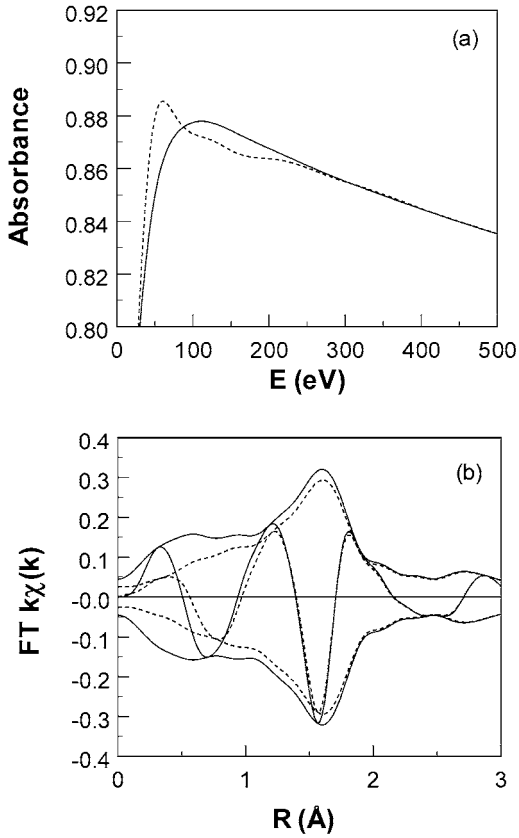

Figure 6. (a) Backgrounds for experimental $Na_2Pt(OH)_6$ data obtained using the indicated S_m values. Note the scale: data have not been normalized. Solid curve, DEE in oscillatory part ($SM_{R=0.0}$); dashed curve, DEE in background ($SM_{R<0.5}$). (b) k weighted FTs (k = 2.5–15 Å^{-1}) corresponding to XAFS spectra remaining after removing background signals shown in (c).

references provided an optimal fit to the first coordination shell of the experimental, background subtracted XAFS spectra for both Pt foil [17] and $Na_2Pt(OH)_6$ [18].

In the XDAP code the Debye–Waller factor is given as an offset (i.e. $\Delta\sigma^2 = \sigma^2_{\text{sample}} - \sigma^2_{\text{ref}}$) with respect to the reference. The Debye–Waller parameter in FEFF7 was optimized so that the offset in the Debye–Waller factor from XDAP is approximately zero. The value of ${S_0}^2$ was determined by assuring that the first shell fit results in the correct coordination number for both samples. The imaginary part of the potential, V_i, takes into account the experimental broadening, so it was determined to give the optimal fit to the width of the FT peak, which is correlated with the Debye–Waller factor. The real part, V_r, changes the offset in the zero position of the energy E_0 with respect to the absorption edge. The optimal input parameters for FEFF7 obtained in this way are given in table 1, and the fit results in figures 8(a) and (d) for the Pt foil and $Na_2Pt(OH)_6$ respectively. The results of the fit to the experimental spectra with the generated theoretical references are given in table 2.

With optimized theoretical references, it is now possible to separate the FT-AXAFS from the experimental FT-XAFS spectra. Figures 8(b) and (e) display the first shell fits (dotted curve) over a narrower R range. The FT (k weighted) is now also taken over a narrower k range, 2.5 Å^{-1} $< k <$ 8 Å^{-1}. The previous larger k range is reduced to minimize now the

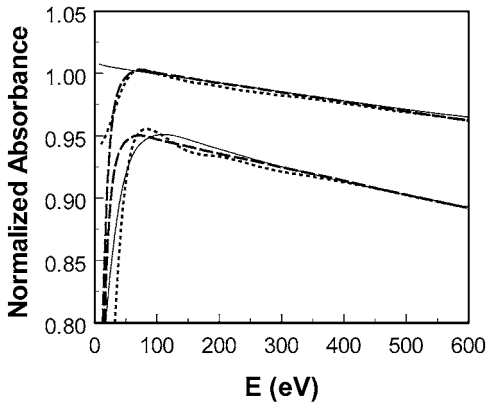

Figure 7. Top: comparison of the free atom background extracted from measured Pt foil data (solid line), Pt_{55} cluster calculation (dotted curve) and calculated free atom absorption (simulated by Pt–H scattering pair at $R = 2.6$ Å, dashed curve). Bottom: similar comparison for free atom experimental Pt–O background (solid curve), PtO_6 cluster (dotted curve) and the same calculated free atom absorption. Lower spectra are shifted for clarity. The experimental free atom backgrounds are obtained by moving both the DEE and AXAFS into the oscillatory part of the XAFS data and removing them fully from the background.

Table 1. Parameters used in the calculations for the generation of the theoretical references.

Atom pair	Potential	σ^2 (Å^2)	S_0^2	V_r (eV)	V_i (eV)
Pt–Pt	Dirac–Hara	0.00234	0.82	−4.2	3.0
Pt–O	Dirac–Hara	0.00342	0.90	0.0	3.0

Table 2. Best fit result for the experimental data using the theoretical references. The fit was performed in R space, k weighted; $\Delta k = 2.5$–15 Å^{-1}, $\Delta R = 1.5$–3.2 Å for Pt foil and $\Delta k = 2.5$–13 Å^{-1}, $\Delta R = 1.3$–1.9 Å for $Na_2Pt(OH)_6$ respectively.

Atom pair	Ncor	R (Å)	$\Delta\sigma^2$ (Å^2)	E_0 (eV)
Pt–Pt	11.68	2.766	−0.00004	0.08
Pt–O	6.14	1.997	−0.00004	4.80

noise contributions in the FT, and no loss of signal occurs since the AXAFS oscillations do not contribute at $k > 8$ Å^{-1}. The fitted first shell Pt–Pt and Pt–O EXAFS functions can now be subtracted from the raw EXAFS data. The solid curves in figures 8(b) and (e) represent the FTs of these difference spectra. A clear AXAFS peak in the FT of the difference spectrum can be distinguished at low R. It can be seen that the FT of the first shell Pt–Pt and Pt–O contribution tails off into the FT AXAFS peak. Due to the shorter distance of the Pt–O absorber–backscattering pair for $Na_2Pt(OH)_6$, the overlap of the peaks of the FT of the first shell Pt–O and the AXAFS is much larger.

The FTs of the difference spectra noted above still contain small contributions from higher shells as is evident in the range $R > 2$ Å. These can be easily removed by Fourier filtering the difference spectra in the range $R = 0.1$–1.5 Å to isolate the FT-AXAFS contributions. The isolated AXAFS (χ_{AX}) is compared with the calculated first shell Pt–Pt and Pt–O (χ_{EX}) EXAFS in figures 8(c) and (f), respectively.

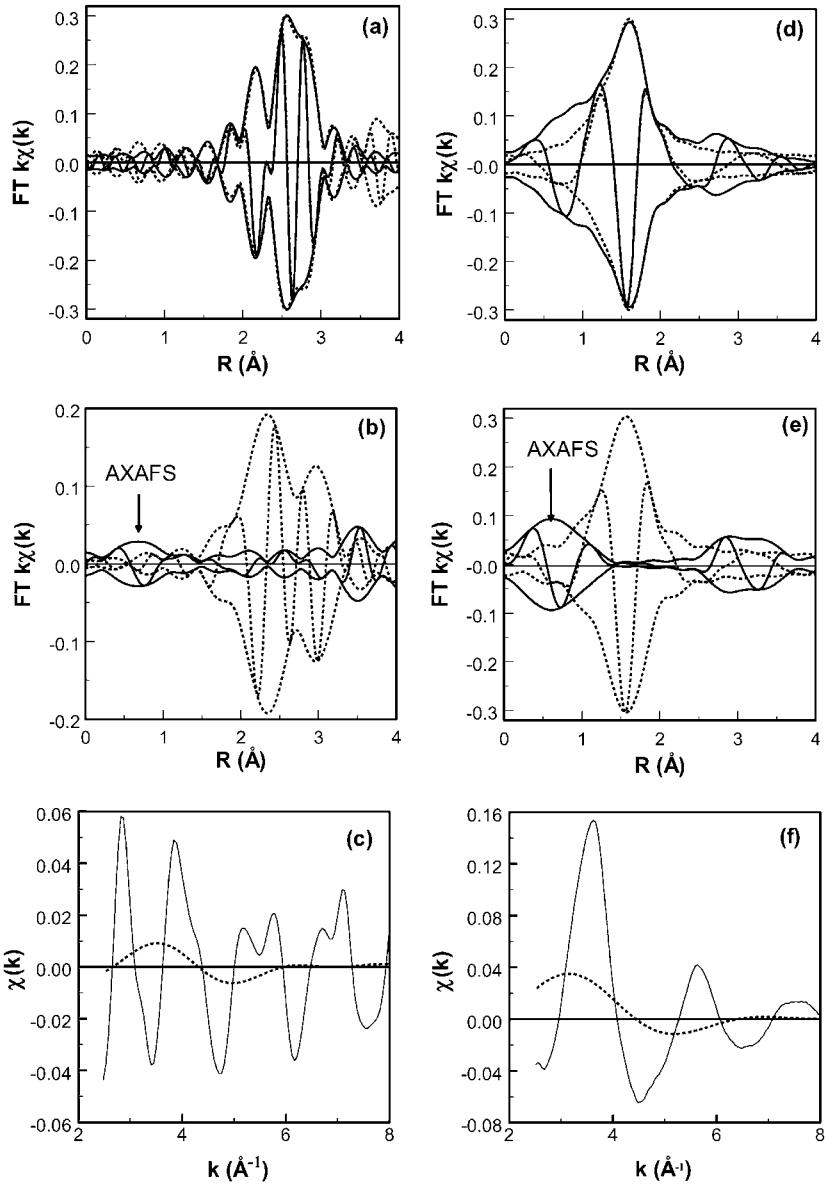

Figure 8. (a) FT (k^1, $\Delta k = 2.5$–15 Å^{-1}) of the experimental XAFS (solid curve) and the first shell Pt–Pt fit (dotted curve) for Pt foil. (b) FT (k^1, $\Delta k = 2.5$–10 Å^{-1}) of the first shell Pt–Pt fit (dashed curve) and the difference file (experimental XAFS minus first shell Pt–Pt fit) (solid curve) for Pt foil. (c) Isolated AXAFS (FT, k^1, $\Delta k = 2.5$–10 Å^{-1}; FT^{-1}, $\Delta R = 0.2$–1.7 Å) (dotted curve) and experimental XAFS (solid curve). (d) FT (k^1, $\Delta k = 2.5$–13 Å^{-1}) of the experimental XAFS (solid curve) and first shell Pt–O fit (dashed curve) for $Na_2Pt(OH)_6$. (e) FT (k^1, $\Delta k = 2.5$–10 Å^{-1}) of the first shell Pt–O fit (dashed curve) and difference file (experimental XAFS minus first shell Pt–O fit) for $Na_2Pt(OH)_6$. (f) Isolated AXAFS (FT, k^1, $\Delta k = 2.5$–10 Å^{-1}; FT^{-1}, $\Delta R = 0.3$–1.5 Å) (dotted curve) and experimental XAFS (solid curve).

4. Discussion

Figure 2 makes clear that by using an SM value around 2.7 the historically used background criterion $SM_{R<1.5}$ indeed can minimize the low R peaks in the FT but with a loss in intensity of the

first shell Pt–Pt peak of about 10%. This study also confirms that the $SM_{R<0.5}$ criterion used in our previous papers dealing with the study of AXAFS leaves the AXAFS contribution in the oscillatory part of the spectrum. Further, figure 1 reveals a good separation between the structure below $R = 0.5$ Å and the AXAFS and regular EXAFS structure, since this low R structure is totally removed well before significant reduction of the higher structure appears. By a systematic variation of the SM parameter, it has been shown that the 0.2 Å feature in the FT visible with SM equal to 3.2 produces a steplike function in the background for SM values higher than 3.4.

Utilization of an analytical expression to model the contribution of DEEs in the XAS spectrum for Pt foil, and variation of the parameters in this expression, verify that the peak around 0.2 in the experimental FT is caused by the DEE with only a small contribution appearing around 0.8 Å. This suggests that our background criterion is generally applicable to separate the DEE and AXAFS contributions. In reasonable agreement with the calculations by Di Cicco and Filipponi (110 eV), we find that the onset for the DEE is at approximately 140 eV.

As can be seen in figure 1(b), removal of the DEE causes a very small loss in AXAFS intensity: compare the dotted curve (SM = 3.5) with the solid curve (SM = 3.4). The DEE peak is completely removed from the FT, while the intensity of the first shell Pt–Pt peak decreased by only 0.04% when using the optimal value, SM = 3.4. It appears that it is indeed possible to separate the DEE and AXAFS contributions with an appropriate criterion for SM. Surprisingly, a very small fraction (0.04%) of the very large Pt–Pt EXAFS appears in the background already at $SM_{R<0.5}$, but this certainly does not cause any problems with the AXAFS analysis, and in fact the $SM_{R<0.5}$ criterion is a major improvement on the traditional criterion, $SM_{R<1.5}$, for analysing the Pt–Pt EXAFS.

This work reveals the importance of utilizing a continuous smoothing parameter, SM, which enables complete control over the extent of smoothing and hence the ability to carefully apply the $SM_{R<0.5}$ criterion. Such a capability exists in some commercial EXAFS analysis programs such as XDAP [16] used here, but not in most of the others. The more usually applied nodal spline technique [19] allows only a choice of integer (i.e. number of nodes), which does not allow the flexibility to carefully dictate the $SM_{R<0.5}$ criterion. It is then nearly impossible to carry out the careful DEE/AXAFS separation performed here.

Finally, the AXAFS contributions have strong overlap with the first shell Pt–Pt and Pt–O EXAFS contributions. The AXAFS can be separated from these EXAFS contributions using the 'difference file' technique with fitting in R space using the same procedure as developed to separate the AXAFS contribution from the XAFS data of small Pt particles dispersed on oxide supports [12]. Figures 8(c) and (f) show that the AXAFS oscillations have a long wavelength and become very small above $k = 8$ Å^{-1}. Although the amplitude of the AXAFS signal is much smaller than the first shell Pt–Pt or Pt–O contribution, it is well above the noise level at low values of k.

5. Conclusions

This study resolves the controversy that existed between the results of Filipponi and Di Cicco [4, 5] and Rehr *et al* [2]. Both DEEs and AXAFS are present in the x-ray absorption spectra of Pt foil and $Na_2Pt(OH)_6$. By performing a careful background subtraction procedure it is possible to leave the DEE features in the background and the AXAFS in the oscillatory part of the spectrum. The importance of having an XAFS data-analysis package that allows for the continuous adjustment of the smooth parameter (SM) in the background subtraction procedure is demonstrated in this study. As already shown by many studies [8–13], the analysis of the isolated FT AXAFS peak makes possible a detailed analysis of the electronic structure of several Pt based electro-chemical and catalytic materials.

References

[1] Holland B W, Pendry J B, Pettifer R F and Bordas J 1978 *J. Phys. C: Solid State Phys.* **11** 633
[2] Rehr J J, Booth C H, Bridges F and Zabinsky S I 1994 *Phys. Rev.* B **49** 12347
[3] Bridges F, Booth C H and Li G G 1995 *Physica* B **208/209** 121
[4] Filipponi A and Di Cicco A 1996 *Phys. Rev.* B **53** 9466
[5] Di Cicco A and Filipponi A 1994 *Phys. Rev.* B **49** 12564
[6] Zabinsky S I, Rehr J J, Ankudinov A, Albers R C and Eller M J 1995 *Phys. Rev.* B **52** 2995
[7] Wende H, Srivastava P, Chauvistré R, May F, Baberschke K, Arvanitis D and Rehr J J 1997 *J. Phys.: Condens. Matter* **9** L427
[8] O'Grady W E, Qian X and Ramaker D E 1997 *J. Phys. Chem.* B **101** 5624
[9] Ramaker D E, Mojet B L, Koningsberger D C and O'Grady W E 1998 *J. Phys.: Condens. Matter* **10** 8753
[10] Mojet B L, Miller J T, Ramaker D E and Koningsberger D C 1999 *J. Catal.* **186** 15
[11] Koningsberger D C, de Graaf J, Mojet B L and Ramaker D E 2000 *Appl. Catal.* **191** 205
[12] Ramaker D E, van Dorssen G E, Mojet B L and Koningsberger D C 2000 *Top. Catal.* **10** 157
[13] Ramaker D E, Qian X and O'Grady W E 1999 *Chem. Phys. Lett.* **299** 221
[14] Vaarkamp M, Miller J T, Modica F S and Koningsberger D C 1996 *J. Catal.* **163** 294
[15] Cook J W and Sayers D E 1981 *J. Appl. Phys.* **52** 5024
[16] Vaarkamp M, Linders J C and Koningsberger D C 1995 *Physica* B **208/209** 159
[17] Wyckoff R W G 1963 *Crystal Structures* vol 1, 2nd edn (New York: Wiley) p 10
[18] Trömel M and Lupprich E 1975 *Z. Anorg. Chem.* **160** 414
[19] Press W H, Flannery B P, Teukolsky S A and Vetterling W T 1989 *Numerical Recipes in C* (Cambridge: Cambridge University Press)